Society For Biomaterials

Microparticulated and nanoparticulated zirconium oxide added to calcium silicate cement: Evaluation of physicochemical and biological properties

Guilherme F. Silva,[1] Roberta Bosso,[1] Rafael V. Ferino,[1] Mário Tanomaru-Filho,[1] Maria I. B. Bernardi,[2] Juliane M. Guerreiro-Tanomaru,[1] Paulo S. Cerri[3]

[1]Department of Restorative Dentistry, Dental School - Araraquara, UNESP (Univ. Estadual Paulista), Araraquara, SP, Brazil
[2]Grupo Crescimento de Cristais e Materiais Cerâmicos, Physics Institute of São Carlos, University of São Paulo - USP, São Carlos, SP, Brazil
[3]Laboratory of Histology and Embryology, Araraquara Dental School, UNESP (Univ. Estadual Paulista), Araraquara, SP, Brazil

Received 1 August 2013; revised 10 January 2014; accepted 28 January 2014
Published online 20 February 2014 in Wiley Online Library (wileyonlinelibrary.com). DOI: 10.1002/jbm.a.35099

Abstract: The physicochemical and biological properties of calcium silicate-based cement (CS) associated to microparticulated (micro) or nanoparticulated (nano) zirconium oxide (ZrO_2) were compared with CS and bismuth oxide (BO) with CS. The pH, release of calcium ions, radiopacity, setting time, and compression strength of the materials were evaluated. The tissue reaction promoted by these materials in the subcutaneous was also investigated by morphological, immunohistochemical, and quantitative analyses. For this purpose, polyethylene tubes filled with materials were implanted into rat subcutaneous. After 7, 15, 30, and 60 days, the tubes surrounded by capsules were fixed and embedded in paraffin. In the H&E-stained sections, the number of inflammatory cells (ICs) in the capsule was obtained. Moreover, detection of interleukin-6 (IL-6) by immunohistochemistry and number of IL-6 immunolabeled cells were carried out. von Kossa method was also performed. The differences among the groups were subjected to Tukey test ($p \leq 0.05$). The solutions containing the materials presented an alkaline pH and released calcium ions. The addition of radiopacifiers increased setting time and radiopacity of CS. A higher compressive strength in the CS + ZrO_2 (micro and nano) was found compared with CS + BO. The number of IC and IL-6 positive cells in the materials with ZrO_2 was significantly reduced in comparison with CS + BO. von Kossa-positive structures were observed adjacent to implanted materials. The ZrO_2 associated to the CS provides satisfactory physicochemical properties and better biological response than BO. Thus, ZrO_2 may be a good alternative for use as radiopacifying agent in substitution to BO. © 2014 Wiley Periodicals, Inc. J Biomed Mater Res Part A: 102A: 4336–4345, 2014.

Key Words: calcium silicate cement, physicochemical properties, biocompatibility, radiopacifying agents

How to cite this article: Silva GF, Bosso R, Ferino RV, Tanomaru-Filho M, Bernardi MIB, Guerreiro-Tanomaru JM, Cerri PS. 2014. Microparticulated and nanoparticulated zirconium oxide added to calcium silicate cement: Evaluation of physicochemical and biological properties. J Biomed Mater Res Part A 2014:102A:4336–4345.

INTRODUCTION

Mineral trioxide aggregate (MTA) has been widely recommended in dentistry for pulp capping, pulpotomy, apical barrier formation in teeth with necrotic pulps and open apexes, repair of root perforations, and root-end filling due to its marginal adaptation and biocompatibility.[1,2] This material is basically composed by Portland cement (PC), a calcium silicate-based material (CS) added to a radiopacifying agent, bismuth oxide (BO), in a 4:1 proportion.[3] It has been reported that PC exhibits biocompatibility and high compressive strength allowing that this material may be also suitable for medical indications, such as in orthopedic applications.[4]

Studies have been demonstrated that the addition of 20% BO to PC confers high radiopacity[5–7] but interferes in some properties of the material.[8–10] Evidence suggests that BO interferes with the hydration mechanism of MTA and precipitation of calcium hydroxide in the hydrated paste.[9] Furthermore, the association of BO dramatically changes the microstructure of the cement by acting as flaws within the cement matrix[8] and, consequently, increases the porosity and solubility of the PC culminating in the reduction of its resistance.[8–11] Regarding the biocompatibility, it has been shown that BO interferes with cell growth[12] and, in human dental pulp cell cultures, increases the cytotoxicity of the material.[13]

Correspondence to: P. S. Cerri; e-mail: pcerri@foar.unesp.br
Contract grant sponsor: CNPq, FUNDUNESP; contract grant number: Proc. n° 01054/11-DFP
Contract grant sponsor: FAPESP; contract grant number: 2010/10769-1

So, other high molecular mass materials have been studied as alternatives radiopacifiers agents[5–7,14] to be added to MTA. One of these materials is zirconium oxide (ZrO_2) which was initially introduced as a biomaterial in orthopedic surgery due to its hardness, high density, and good wear resistance. More recently, it has been related that ZrO_2 added to PC in a 1:4 ratio provides an adequate radiopacity, that is, superior to the recommended by ISO 6876 specification for dental root canal sealing materials.[5,6] There is evidence that this mixture releases calcium ions and provides to the microenvironment an alkaline pH.[7] Moreover, studies have been shown that the addition of 30% ZrO_2 does not affect the hydration reaction of PC and originates a bioactive cement[15] with comparable properties with MTA.[14]

It has been suggested that the reduction in the material particle size could improve the physicochemical properties of MTA due to its rapid hydration.[16] MTA-based material composed by small particles exhibits reduced setting time and increased microhardness.[17] It has been demonstrated that ZrO_2, in its nanoparticulated form, presents bioactivity, cytocompatibility,[18] and high resistance.[19] However, the effects of nanoparticulated ZrO_2 on the properties of CSs are unknown.

Thus, the aim of this study was to evaluate some physicochemical properties such as pH, release of calcium ions, radiopacity, setting time, and compression strength of a CS, PC, associated to 30% microparticulated or nanoparticulated ZrO_2 in comparison with CS and CS added to BO. Furthermore, the tissue reaction promoted by these materials in the rat subcutaneous was investigated by morphological, immunohistochemical, and quantitative analyses.

MATERIALS AND METHODS

In this study, the following materials were tested: CS (White Portland cement; CPB-40—Votorantin Cimentos, Camargo Correa S.A., Pedro Leopoldo, MG, Brazil), CS group; CS with BO (Sigma Aldrich, St. Louis, MO), CS + BO group; CS with microparticulated ZrO_2 (Sigma Aldrich, St. Louis, MO), CS + ZrO_2 micro group and CS with nanoparticulated ZrO_2, CS + ZrO_2nano group. The powder (CS, CS + BO, CS + ZrO_2 micro, and CS + ZrO_2nano) was previously sterilized by ultraviolet method for 30 min. A ratio of 20% BO and 80% CS and 30% ZrO_2 and 70% CS by weight were used for analyses. The materials were mixed at a ratio of 1 g powder of cement per 0.3 mL liquid (distilled water) as previously described.[5,7,13,14] Regarding to CS + ZrO_2, it has been demonstrated that this powder/liquid proportion provides a material with comparable properties to MTA[14] and does not interfere in the hydration reaction of calcium silicate cement.[15] Moreover, the CS + ZrO_2nano was prepared using a powder:liquid mixing ratio of 1 g:0.33 mL, standardized in pilot tests, because it provided a thicker consistency to the nanoparticulated cement in comparison to the other materials, easier to handle, and to insert in the polyethylene tubes. Thus, this proportion provided an adequate handling and consistency characteristics for a cement intended for use as a root-end filling material. Nanoparticulated ZrO_2 was performed by polymeric precursor method at Institute of Physics of São Carlos (University of São Paulo, São Carlos, Brazil); the particle size obtained was 74 nm which was confirmed by Brunauer-Emmett-Teller surface area analysis.

Analyses of the pH and calcium ion release

The pH and calcium ion release were evaluated according to methodology performed by Vivan et al.[20] and Duarte et al.[7] Ten polyethylene tubes (Embramed Ind. Com., São Paulo, SP, Brazil) measuring 10.0 mm length and 1.6 mm diameter were filled with freshly prepared samples of each material, sealed in flasks containing 10 mL of distilled water, and stored at 37°C. After 1 day of immersion, the tubes were carefully removed and placed into new flasks with an equal amount of distilled water, and this procedure was repeated after 7, 14, and 28 days. The solutions pH was analyzed at each period using a previously calibrated digital pH meter (Ultrabasic; Denver Instrument Company, Arvada, CO). The same solutions used to test pH were used to test for calcium ion release. At the same periods, the calcium ions released in the distilled water was measured using an atomic absorption spectrophotometer (H1170 Hilger & Watts; Rank Precision Industries, Analytical Division, London, UK). The concentration of calcium ions released from the materials was quantified using a calcium hollow cathode lamp (422.7-nm wavelength and 0.7-nm window) operated at 20 mA. The readings of calcium ion release were compared with a standard curve obtained from multiple dilutions of pure calcium in ultrapure water.

Radiopacity

The specimens used for radiopacity test were prepared according to the ISO 6876/2001[21] standard for dental root-sealing materials. Five specimens, measuring 10 mm diameter by 1.0 mm thickness, were made for each tested material. The specimens were stored at 37°C for 24 h, and subsequently, they were positioned on five occlusal radiographic films (Insight-Kodak Comp, Rochester, NY) and exposed, along with an aluminum stepwedge with variable thickness (from 2 to 16 mm, in 2-mm increments) as described by Bortoluzzi et al.[5] and Duarte et al.[6] A GE-1000 X-ray unit (General Electric, Milwaukee, WI) operating at 50 kVp, 10 mA, 18 pulses/s, and focus-film distance of 33.5 cm was used. The films were processed in a standard automatic processor (Dent-X 9000, Dent-X, Elmsford, USA). Radiographs were digitized using a desktop scanner (SnapScan 1236-Agfa, Deutschland) and the digitized images were imported to the Image Tool 3.0 (UTHSCSA, San Antonio, TX); an equal-density tool was used to identify equal-density areas in the radiographic images.[5,6] This procedure allowed comparison between the radiographic density of the cements and the radiopacity of the different aluminum stepwedge thicknesses. The area corresponding to the specimen was selected in each radiographic image to verify the thickness of the aluminum stepwedge detected by the software as equivalent to the material's radiographic density. Thus, the radiopacity of the evaluated materials was estimated from the thickness of aluminum (in mm) by using a

conversion equation.[6] The values recorded for each material were averaged to obtain a single value in mm Al.

Setting time

This test was carried out as determined by #57 of American Dental Association[22] and C266-03 of American Society for Testing and Materials.[23] Six specimens measuring 10 mm diameter and 2 mm in height were made per each material. At 120 ± 10 s after the onset of mixture, the assembly was placed in a well-sealed plastic flask and stored in an oven at 37°C and 95% relative humidity. After 150 ± 10 s to the onset of mixture, a Gilmore needle of 100 ± 0.5 g and active tip of 2.0 ± 0.1 mm diameter was vertically placed on the cement surface. This procedure was repeated at 60-s intervals. The initial setting time of the cement was considered as the time between the onset of mixture and the moment when the marks of needles could not be observed on the cement surface. Concerning the final setting time, a Gilmore needle of 456 ± 0.5 g and active tip of 1.0 ± 0.1 mm diameter were used as previously described. The initial and final setting times were determined by the arithmetic mean of six repetitions of the test for each group.[24]

Compression strength

To test the compression strength, specimens measuring 12 mm in height by 6 mm in diameter were made according to ISO 9917-1/2003.[25] Six specimens were used in each group; these specimens were maintained at 37°C under 100% relative humidity until the tests were performed. The specimens were subjected to testing at 24 h, 7, 14, 21, and 28 days after-manipulation of the cements[10] using an universal testing machine (EMIC DL 2000, Curitiba, PR, Brazil), at a speed of 0.5 mm/min and load of 5 kN. All measurements were recorded in kg and converted to megapascal (MPa).

Tissue reaction

The research protocol on animal use of this study was authorized by the Ethical Committee for Animal Research of the São Paulo State University, Brazil (CEUA n° 26/2010-Araraquara Dental School-UNESP). Sixty male Holtzman rats (*Rattus norvegicus albinus*) weighing 250 ± 10 g were used. The rats were maintained in individual stainless steel cages under a 12:12 light-dark cycle at a controlled temperature (23 ± 2°C) and humidity ($55 \pm 10\%$), with food and water provided *ad libitum*.

The animals were distributed into five groups according the evaluated materials ($n = 5$ per group in each period). The polyethylene tubes (Embramed Ind. Com., Sao Paulo, SP, Brazil) with 10.0 mm length and 1.6 mm diameter, previously sterilized with ethylene oxide, were filled with CS (CS group), CS with BO (CS + BO group), CS with microparticulated ZrO_2 (CS + ZrO_2micro group) or CS with nanoparticulated ZrO_2 (CS + ZrO_2nano group), and control group (CG), empty polyethylene tubes. After mixing of the materials, the polyethylene tubes were filled and immediately implanted into the dorsal subcutaneous. In each rat, two polyethylene tubes, filled with different materials each, were implanted in the subcutaneous; in control group (CG), two empty polyethylene tubes were placed in the subcutaneous. Thus, five polyethylene tubes were analyzed per group in each experimental period.

The animals were anesthetized with an intraperitoneal injection of ketamine (80 mg/kg of body weight) combined with xylazine (4 mg/kg of body weight). The dorsal skin was shaved and disinfected with 5% iodine solution. Subsequently, a 20-mm-long incision was made using a scalpel (n° 15, Fibra Cirurgica, Joinvile, SC, Brazil) and two polyethylene tubes, each filled with one of the materials, were placed into the subcutaneous pockets. After 7, 15, 30, and 60 days of implantation, the tubes surrounded by connective tissue were removed and the specimens were processed for paraffin embedding. The analysis at 7 and 15 days was conducted to evaluate the initial reaction induced by materials as well as the kind of inflammatory cells (ICs) observed in the capsules. The prolonged periods (30 and 60 days) were used to evaluate if the materials implanted allow that ICs would be replaced by fibroblasts and collagen fibers.

Histological procedures

The specimens were fixed in 4% formaldehyde (prepared from paraformaldehyde) buffered at pH 7.2 with 0.1*M* sodium phosphate for 48 h at room temperature. Subsequently, the specimens were dehydrated and embedded in paraffin. Longitudinal sections, 6 μm thick, were stained with hematoxylin & eosin (H&E) for morphological analysis. H&E-stained sections were also used to estimate the number of ICs in the capsule. Sections were submitted to the von Kossa histochemical method, for detection of calcified structures in the connective tissue adjacent to the implanted materials. Sections were also adhered to silanized slides for interleukin-6 (IL-6) immunohistochemical reaction.

Numerical density of inflammatory cells. The numerical density of ICs was undertaken using a light microscope (BX51, Olympus, Tokyo, Japan) and an image analysis system (Image Pro-Express 6.0, Olympus) as previously described.[26] In each implant, three H&E-stained sections of the capsule were selected at intervals of at least 100 μm. In each section, a standardized field 0.09 mm^2 of the capsule adjacent to the opening of the tube implanted was analyzed, totaling 0.27 mm^2 per implant. In each area, the total number of IC (neutrophils, lymphocytes, plasma cells, and macrophages) was counted using the image analysis system at 695× magnification. Thus, the number of ICs/mm^2 was obtained for each implant.

Interleukin-6 immunohistochemistry. For antigen retrieval, deparaffinized sections were immersed in 0.001*M* sodium citrate buffer pH 6.0 and maintained at 90–94°C for 20 min in a microwave oven. After a cooling-off period, the sections were washed and the endogenous peroxidase was blocked with 5% hydrogen peroxide for 20 min. After washings in 0.1*M* sodium phosphate buffer (PBS) at pH 7.2, the sections were incubated with 2% bovine serum albumin (Sigma-Aldrich Chemie, Germany) for 30 min. Subsequently, the sections were incubated overnight at 4°C with anti-IL-6 goat

TABLE I. Means and Standard Deviations of pH Values and Calcium Ion Release (mg/L) for the Different Materials in the Evaluation Periods

	CS	CS + BO	CS + ZrO_2micro	CS + ZrO_2nano
1 Day				
pH	10.36 (0.32)[a]	10.31 (0.29)[a]	10.41 (0.33)[a]	10.38 (0.35)[a]
Calcium	3.13 (1.47)[a]	2.73 (0.70)[a]	2.44 (0.43)[a]	2.44 (0.43)[a]
7 Days				
pH	10.29 (0.09)[a]	9.66 (0.53)[b]	10.15 (0.39)[a]	10.24 (0.21)[a]
Calcium	11.92 (0.83)[a]	7.74 (1.01)[b]	11.00 (1.46)[a]	10.61 (1.26)[a]
14 Days				
pH	9.88 (0.17)[a]	9.53 (0.41)[b]	9.84 (0.29)[a]	9.94 (0.22)[a]
Calcium	10.90 (1.83)[a]	9.12 (0.90)[b]	12.74 (2.10)[a]	11.77 (2.03)[a]
28 Days				
pH	9.88 (0.06)[a]	9.32 (0.21)[b]	9.72 (0.28)[a]	9.97 (0.35)[a]
Calcium	11.61 (3.26)[a]	8.06 (1.32)[b]	9.19 (1.07)[a]	9.11 (1.20)[a]

The different superscript letters (a and b) in the lines indicate significant differences among materials ($p \leq 0.05$).

primary antibody (Santa Cruz Biotechnology, USA), diluted 1:400. After washings in PBS, the immunoreaction was detected by the Labeled StreptAvidin-Biotin system (LSAB-plus Kit; Dako, USA). After incubation for 20 min at room temperature with multilink solution containing biotinylated mouse/rabbit/goat antibodies, the sections were washed in PBS and subsequently were incubated with streptavidin-peroxidase complex for 20 min at room temperature. Peroxidase activity was revealed by Betazoid DAB (Biocare Medical, USA) for 3 min; the sections were counterstained with Carazzi's hematoxylin. As negative controls, the primary antibody was replaced by non-immune serum.

Numerical density of IL-6-immunolabeled cells. The number of IL-6-immunolabeled cells per mm^2 of the capsule was counted at 695× using an image analysis system (Image Pro-Express 6.0, Olympus) following the methodology previously described.[27] For each tube implanted, the IL-6 positive cells were counted in a standardized area (0.09 mm^2); in each group ($n = 5$), the values were divided by the total area, and then, the number of IL-6/mm^2 was obtained.

von Kossa histochemical reaction. The von Kossa method was used for detection of calcified structures[26,28] in the capsule formed on the opening tube. Three sections per implant were selected at intervals of at least 100 μm. Deparaffinized sections were immersed in 5% silver nitrate solution for 1 h; the sections were washed in distilled water and subsequently were immersed in 5% sodium thiosulfate for 5 min. After washings, the sections were stained by picrosirius method and mounted in resinous medium. As negative control, some sections were immersed in 10% EDTA solution and subsequently submitted to the von Kossa method. As positive control, the sections of tibiae of young rats were used.

Statistical analysis

The differences between the groups were statistically analyzed by the SigmaStat 2.0 software (Jandel Scientific, Sausalito, CA). The data of all physicochemical tests and of the morphometrical findings were submitted to ANOVA and Tukey test. The significance level accepted was $p \leq 0.05$.

RESULTS

Analyses of the pH and calcium ion release

The pH solutions of the materials varied from 9.32 to 10.41 in the periods. At 1 day, statistical differences were not found among materials; however, the pH of solutions containing CS + BO was significantly smaller in comparison with other groups at 7, 14, and 28 days (Table I).

According to Table I, a significant increase in the amount of calcium released was observed from the 1 to 7 days in all materials. The amount of calcium ion released by CS + BO was significantly lower in comparison with other materials at 7, 14, and 28 days.

Radiopacity and setting time

The radiopacity of CS + OB, CS + ZrO_2micro, and CS + ZrO_2nano was significantly higher than CS; differences between the CS + OB, CS + ZrO_2micro, and CS + ZrO_2nano materials were not statistically significant. Statistical differences in the initial and final setting times were not found among CS + ZrO_2micro, CS + ZrO_2nano, and CS + OB materials; otherwise, the CS exhibited significantly shorter initial and final setting times in comparison with other groups (Table II).

TABLE II. Means and Standard Deviations of Radiopacity (mm Al) for the Initial and Final Setting Times (in min) for Each Material

		Setting Time	
Materials	Radiopacity	Initial	Final
CS	1.32 (0.09)[a]	31.0 (3.2)[a]	120.2 (2.4)[a]
CS + BO	4.45 (0.37)[b]	38.5 (4.3)[b]	167.8 (4.9)[b]
CS + ZrO_2micro	4.12 (0.34)[b]	45.5 (3.3)[b]	175.8 (7.0)[b]
CS + ZrO_2nano	4.12 (0.23)[b]	48.8 (5.7)[b]	169.0 (9.0)[b]

Different superscript letters (a and b) indicate statistically significant differences ($p < 0.05$).

TABLE III. Means and Standard Deviations for Compressive Strength Values (in MPa) at 24 h, 7, 14, 21, and 28 Days After Manipulation of Each Material

	CS	CS + BO	CS + ZrO_2micro	CS + ZrO_2nano
24 h	41.22 (3.40)^{a,1}	10.96 (1.53)^{b,1}	34.23 (3.47)^{c,1}	31.50 (4.23)^{c,1}
7 Days	49.88 (1.02)^{a,2}	18.86 (4.10)^{b,2}	41.06 (2.10)^{c,2}	40.20 (2.60)^{c,2}
14 Days	51.63 (2.70)^{a,2}	21.05 (4.13)^{b,2}	42.76 (2.54)^{c,2}	41.16 (2.00)^{c,2}
21 Days	63.29 (4.90)^{a,3}	21.82 (3.29)^{b,2}	48.93 (3.33)^{c,3}	50.44 (5.49)^{c,3}
28 Days	64.38 (2.90)^{a,3}	27.95 (4.03)^{b,3}	49.15 (1.51)^{c,3}	50.56 (4.01)^{c,3}

Different superscript letters (a–c) in the lines indicate statistically significant difference amongst groups ($p < 0.05$).
Different superscript numbers (1–3) in the columns indicate statistically significant difference amongst periods ($p < 0.05$).

Compression strength

In all periods, CS material exhibited the highest compression strength values compared with other groups. The lowest compression strength means were found in CS + BO material; statistical differences between CS + ZrO_2micro and CS + ZrO_2nano groups were not detected. In all groups, an

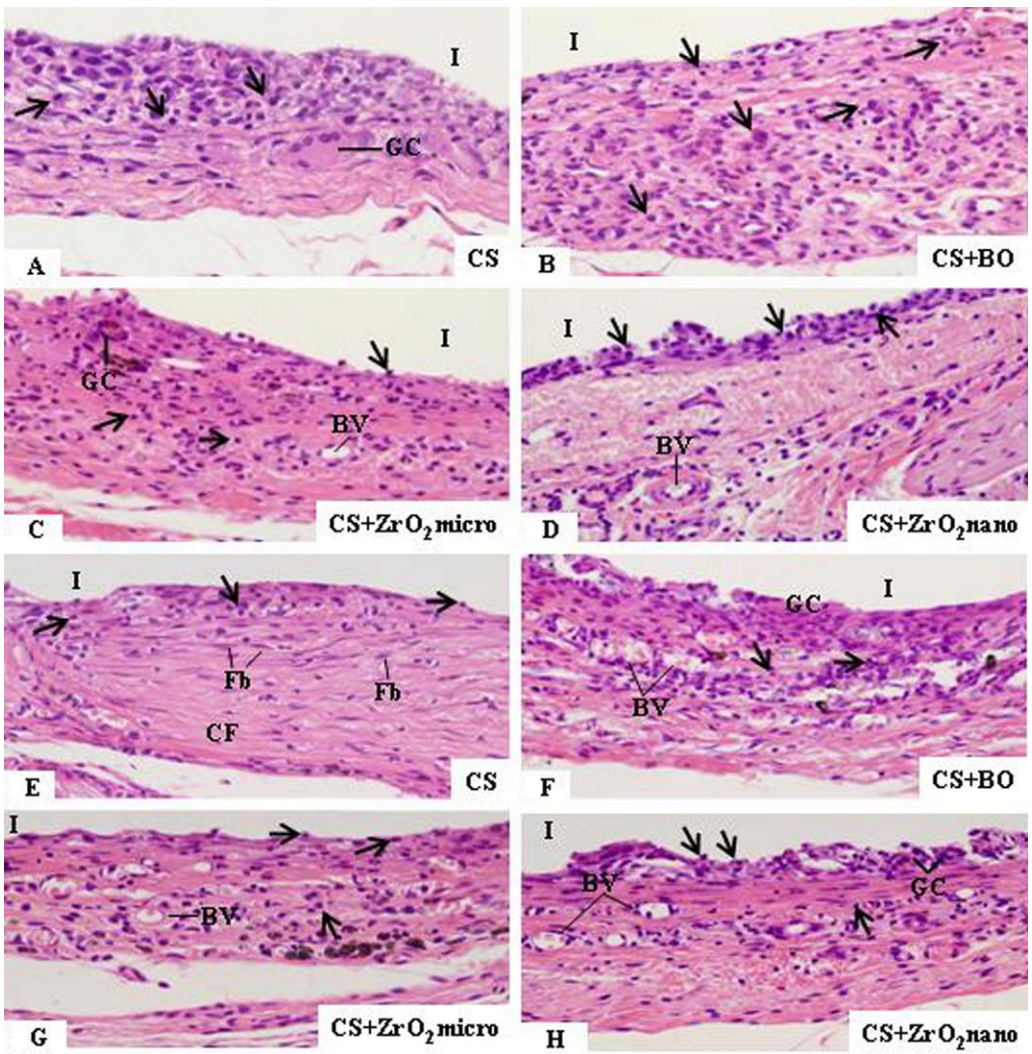

FIGURE 1. A–H: Light micrographs of sections showing portions of capsule adjacent to the opening of the tubes implanted (I) in the subcutaneous tissue of the CS (A and E), CS + BO (B and F), CS + ZrO_2micro (C and G), and CS + ZrO_2nano (D and H) groups at 7 days (A–D) and 15 days (E–H). A (CS): Several inflammatory cells (arrows) are seen, mainly, in the inner portion of the capsule adjacent to CS. GC, giant cell. ×200. B (CS + BO): Numerous inflammatory cells (arrows) are distributed by throughout capsule. ×200. (C) (CS + ZrO_2micro) and (D) (CS + ZrO_2nano): The capsules show several inflammatory cells (arrows). Note that in the CS + ZrO_2nano group, the inflammatory cells (arrows) are present, mainly, in the inner portion of the capsule in close juxtaposition to material (I). (BV), blood vessels. ×190. E (CS): The capsule is composed by fibroblasts (Fb) amongst the collagen fibers (CF); the inflammatory cells (arrows) are seen in the inner portion of the capsule. ×190. (F) (CS + BO), (G) (CS + ZrO_2micro), and (H) (CS + ZrO_2nano): The capsules exhibit several inflammatory cells (arrows) and various blood vessels (BV) distributed by the connective tissue. ×190 (F); ×200 (G and H). H&E. [Color figure can be viewed in the online issue, which is available at wileyonlinelibrary.com.]

TABLE IV. Number of Inflammatory Cells (IC) and IL-6 Immunolabeled Cells per mm^2 in the Capsule Adjacent to the Different Materials and Control Group

	CS	CS + BO	CS + ZrO_2micro	CS + ZrO_2nano	Control
7 Days					
IC	531.3 (19.1)^{a,1}	699.6 (6.0)^{b,1}	621.0 (17.1)^{c,1}	626.1 (12.5)^{c,1}	453.9 (7.2)^{d,1}
IL-6	404.4 (6.0)^{a,1}	491.1 (9.2)^{b,1}	408.8 (14.4)^{a,1}	413.3 (14.4)^{a,1}	371.1 (23.0)^{c,1}
15 Days					
IC	409.8 (3.3)^{a,2}	563.4 (6.1)^{b,2}	515.7 (11.1)^{c,2}	514.5 (9.9)^{c,2}	389.4 (12.4)^{d,2}
IL-6	148.8 (20.1)^{a,2}	200.0 (11.1)^{b,2}	168.8 (9.2)^{c,2}	191.1 (9.2)^{b,2}	151.1 (18.5)^{a,2}
30 Days					
IC	374.7 (6.6)^{a,3}	463.5 (17.7)^{b,3}	416.4 (22.2)^{c,3}	425.1 (26.4)^{c,3}	368.4 (13.7)^{a,3}
IL-6	84.4 (6.0)^{a,3}	135.5 (14.4)^{b,3}	102.2 (9.2)^{c,3}	106.6 (6.0)^{c,3}	84.4 (6.0)^{a,3}
60 Days					
IC	197.4 (13.2)^{a,4}	272.1 (8.1)^{b,4}	225.3 (9.0)^{c,4}	229.8 (10.2)^{c,4}	194.7 (16.4)^{a,4}
IL-6	62.2 (2.8)^{a,4}	91.1 (3.1)^{b,4}	62.2 (2.0)^{a,4}	82.2 (0.2)^{c,4}	53.3 (5.4)^{d,4}

The comparison amongst groups ($p < 0.05$) is indicated by different superscript (a–d) in the various lines.
The comparison amongst periods ($p < 0.05$) is indicated by number superscripts in the various columns.
Mean (standard deviation).

increase in the mean values was seen in the periods of 21 and 28 days in comparison with 24 h (Table III).

Tissue reaction

Morphological findings and numerical density of inflammatory cells. At 7 days, a moderate inflammatory process was seen in the capsules juxtaposed to the tubes implanted; this inflammatory process contained mainly lymphocytes and macrophages [Fig. 1(A–D)] and some multinucleated giant cells [Fig. 1(A,C)]. In all groups, the highest numerical density of ICs was verified at 7 days; a gradual and significant reduction in the number of ICs was observed in the subsequent periods (Table IV). At 15 days, the ICs were present in close juxtapotision to the materials implanted as well as next to the blood vessels, except in the CS + BO group; in this group, numerous ICs were still seen dispersed by capsule [Fig. 1(E–H)]. Some multinucleated giant cells were observed in the capsules mainly in close contact to the materials [Fig. 1(F,H)]. On 30 day, the number of ICs was significantly lower in the CS + ZrO_2micro and CS + ZrO_2nano groups in comparison with CS + BO group (Table IV); several macrophages and plasma cells were still present in the capsules of the CS + BO group [Fig. 2(B)]. However, the capsules juxtaposed to the CS + ZrO_2micro and CS + ZrO_2nano did not exhibit collagen fibers as well arranged as observed in CS group [Fig. 2(A–D)]. At 60 days, the capsules frequently exhibited typical bundles of collagen fibers among fibroblasts [Fig. 2(E–H)]. In the CS + BO group, the ICs were present mainly in the innermost portion of the capsule [Fig. 2(F)].

According to Table IV, the highest numerical density of ICs was verified in the capsules adjacent to CS + BO in all periods. In all periods, statistical differences in the number of ICs were not detected between the CS + ZrO_2micro and CS + ZrO_2nano groups; however, these groups exhibited a significant increase in the number of ICs in comparison with the CS group.

Numerical density of IL-6-immunolabeled cells. In all periods, some IL-6 immunolabeled cells were present in the capsules [Fig. 3(A–H)]. According to Table IV, the number of immunolabeled cells was statistically higher at 7 days and, subsequently, a significant and gradual reduction was seen at 15, 30, and 60 days. The highest number of IL-6 positive cells was seen in the capsule of CS + BO group, in all periods. Immunoreaction for IL-6 was not observed in the negative control sections (data not shown).

von Kossa histochemical method. Dense von Kossa-positive structures were often found in the innermost portion of the capsules juxtaposed to the materials implanted, in all periods [Fig. 4(B-H)]; occasionally, small von Kossa-positive structures were dispersed by throughout capsule [Fig. 4(A,D)]. Sections of developing long bone, used as positive control, exhibited black bone trabeculae (von Kossa-positive) in the diaphysis. Moreover, no von Kossa-positive structure was found in the sections used as negative control (data not shown).

DISCUSSION

The results demonstrated that Zr_2O microparticulated or nanoparticulated provides satisfactory physicochemical properties when added to CS. Moreover, the Zr_2O added to the CS exhibited better biological response than association of BO to the CS.

Physicochemical analyses

The evaluated materials with addition of BO or Zr_2O exhibited radiopacity significantly higher than CS and superior to the minimum value recommended by ISO 6876[21] which is in accordance with previous studies.[5,6] Moreover, the means values of calcium ions in the solutions with CS + ZrO_2micro and CS + ZrO_2nano were statistically similar to CS, indicating, therefore, that the addition of 30% micro or nanoparticulated ZrO_2 does not affect the release of calcium ions, as described by other authors.[7,15] Evidence suggests that ZrO_2 does not react with CS, once, the reaction by-products of the ZrO_2 added to the cements did not differ of the pure PC.[15] In contrast, the BO reacts with CS forming a calcium

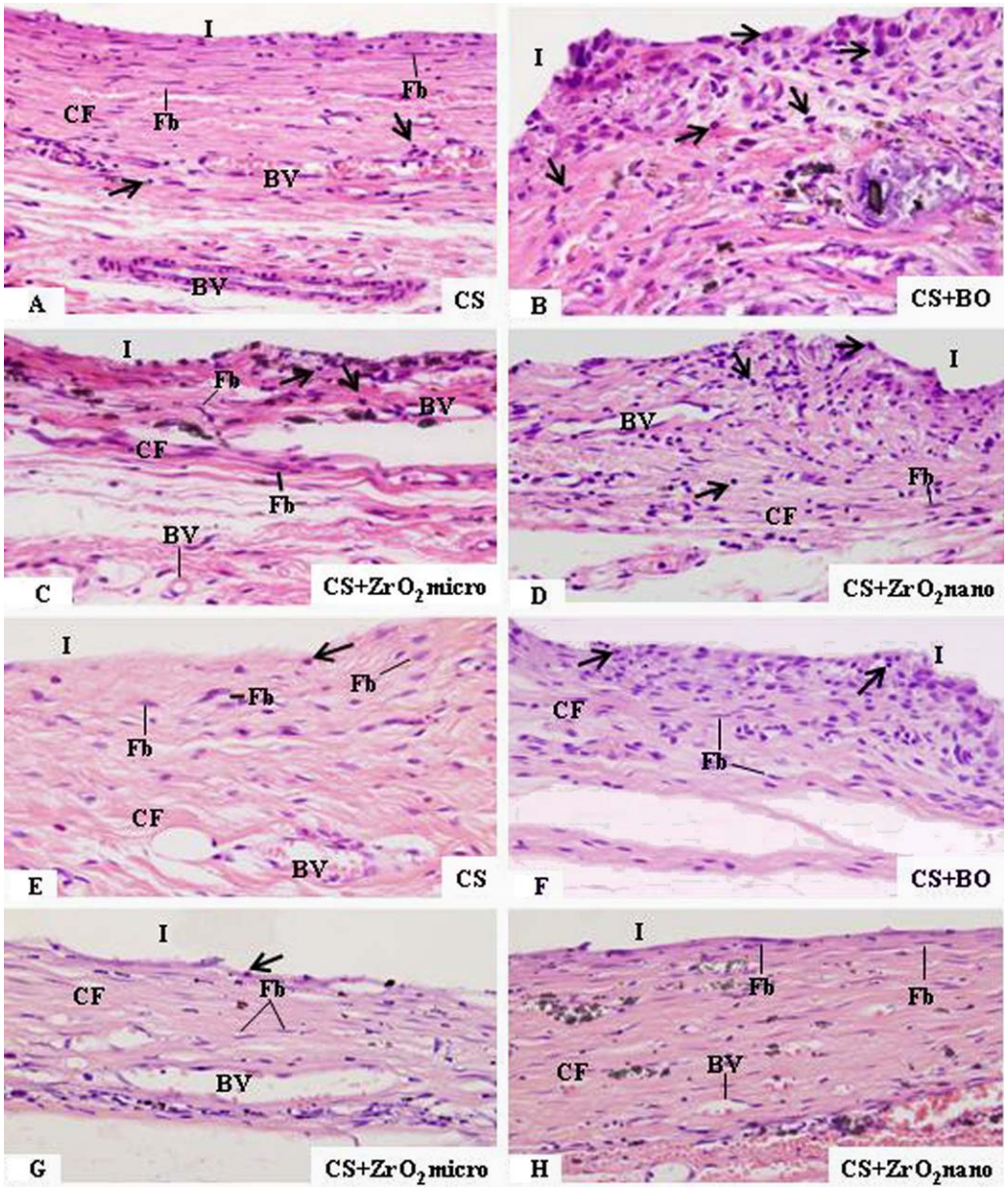

FIGURE 2. A–H: Light micrographs of sections showing portions of capsule adjacent to the opening of the tubes implanted (I) in the subcutaneous tissue of the CS (A and E), CS + BO (B and F), CS + ZrO_2micro (C and G), and CS + ZrO_2nano (D and H) groups at 30 days (A–D) and 60 days (E–H). A (CS): The capsule contains various fibroblasts (Fb) amongst the collagen fiber bundles (CF); the inflammatory cells (arrows) are mainly observed next to the blood vessels (BV). ×190. B (CS + BO): Numerous inflammatory cells (arrows) are presented by throughout of the thick capsule. ×200. (C) (CS + ZrO_2micro) and (D) (CS + ZrO_2nano): The inner portions of the capsules exhibit some collagen fiber bundles (CF) amongst the fibroblasts (Fb); inflammatory cells (arrows) are seen adjacent to the materials implanted (I) and near to the blood vessels (BV). ×200; ×180. E–H: The capsules adjacent to the materials implanted (I) exhibit several fibroblasts (Fb) amongst the collagen fiber bundles (CF); blood vessels (BV) are also present in the connective tissue. Note that evident presence of inflammatory cells (arrows) in the capsule adjacent to CS + BO. ×210 (E); ×190 (F–H). H&E. [Color figure can be viewed in the online issue, which is available at wileyonlinelibrary.com.]

silicate hydrate gel. Our findings showed significant reduction in the amount of release of calcium ions and pH verified in the CS + BO reinforcing the idea that BO interferes with chemical properties of CS. There is evidence that BO reduces the precipitation of calcium hydroxide resulting in low alkalinity of the CS + BO solutions.[9]

The addition of radiopacifiers increased the setting time of CS, as observed in other studies.[7,14] It is possible that the increase in the setting time caused by ZrO_2 (micro and nano) and BO added to CS may be due to the presence of smaller amount of cement in these mixtures, affecting its hydration and increasing the setting time.[9,14] Although significant reduction in the resistance to compression was promoted by ZrO_2 and BO associated to CS cement, the loss of compressive strength caused by ZrO_2 was ~20%, whereas of the BO was around 65% in comparison to pure CS. The BO promotes flaws in the CS matrix formation,[9] causing increase in the porosity and solubility, and, consequently,

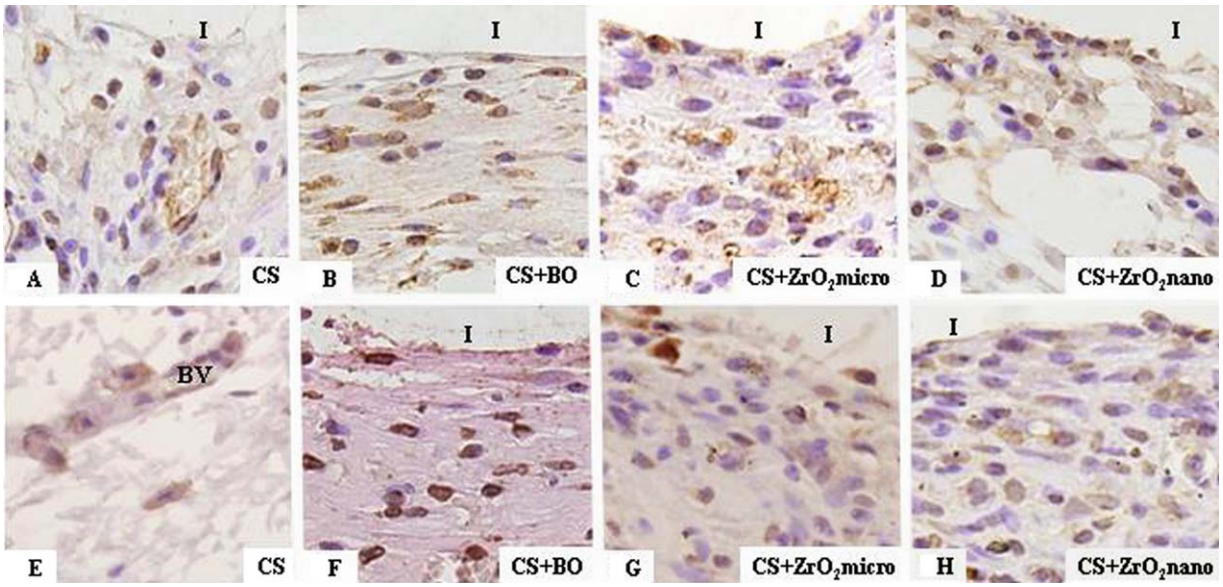

FIGURE 3. A–H: Light micrographs of sections showing portions of capsule adjacent to the opening of the tubes implanted (I) in the subcutaneous tissue at 7 days (A–D) and at 60 days (E–H). The sections were submitted to immunohistochemistry for detection of IL-6 and counterstained by hematoxylin. IL-6-immunolabeling (brown–yellow color) is observed in the cells of the capsule adjacent to the different materials implanted (I). (BV), blood vessel. ×500. [Color figure can be viewed in the online issue, which is available at wileyonlinelibrary.com.]

reduces the mechanical strength of the cement.[8,29] In this study, loss in the compressive strength was also verified in the CS cement associated to 30% ZrO_2. However, no interference in the compressive strength was observed in the addition of 20% ZrO_2 to PC.[10] Considering that PC provides resistance to the material,[8] it is possible that the higher amount of PC present in the mixture could explain these controversial findings. On the other hand, a similar mixture to that used in this study (30% ZrO_2 + CS) did not affect the compressive strength of the CS[14] suggesting that trademark of the ZrO_2 may also interfere in the reaction mechanism.

Our results indicated that microparticulated or nanoparticulated ZrO_2 provides satisfactory physicochemical properties when added to the CS cement and improved the compressive strength of the mixture when compared with

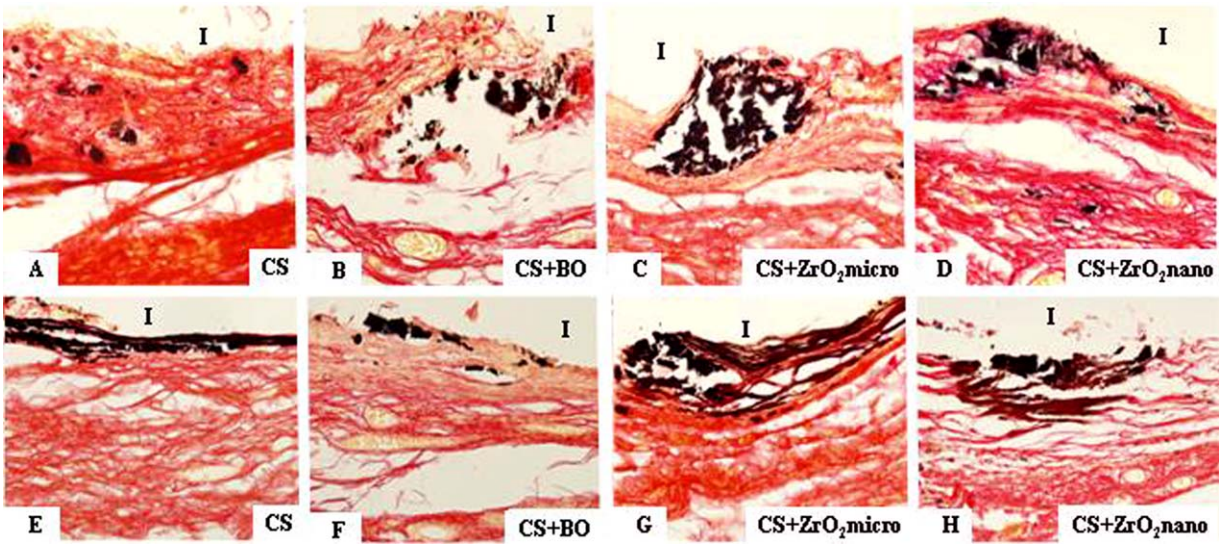

FIGURE 4. A–H: Light micrographs of sections showing portions of capsule adjacent to the opening of the tubes implanted (I) in the subcutaneous tissue at 7 days (A–D) and 60 days (E–H). The sections were submitted to the von Kossa reaction and counterstained by picrosirius. Small and dense von Kossa-positive structures (black color) are dispersed by throughout capsule (A and D). von Kossa-positive structures with irregular-shaped are in the inner portion of the capsules (B–D, G, and H). E: A continuous layer strongly von Kossa-positive is observed in close contact with material. F: Small and dense von Kossa-positive structures are present in the capsule surface. ×220. [Color figure can be viewed in the online issue, which is available at wileyonlinelibrary.com.]

BO. However, statistical significant differences between the values of CS + ZrO_2 (micro and nano) regarding to setting time and increase microhardness were not seen. These findings may be explained at least in part due to the fact that, in this study, microparticulated CS was used. Thus, the reaction of nanoparticulated ZrO_2 to the microparticulated calcium silicate-based material did not provide benefit to the CS in comparison with microparticulated ZrO_2.

Tissue reaction

The morphological and morphometrical findings clearly revealed that ZrO_2 is a radiopacifier agent, which induces lower inflammatory reaction than BO. In all periods, a significant reduction in the number of ICs and IL-6 immunolabeled cells in the capsule juxtaposed to CS associated to ZrO_2 was observed in comparison with CS + BO.

The tubes filled with materials promoted a higher recruitment of ICs than empty tubes indicating, therefore, that these materials may release some substances which stimulate the migration and differentiation of these cells such as macrophages and plasma cells, observed often in the capsules of all materials. During the reaction of CSs, release of hydroxil (OH^-) occurs promoting in the microenvironment an increase in pH (pH around 10). The alkaline pH may stimulate the recruitment of ICs and the production of inflammatory cytokines and chemokines[29] that promote enhancement of leukocyte adhesion to endothelial walls, potentiation of neutrophils, and differentiation of plasma cell.[30,31] Thus, the elevated pH exhibited by CS group may be responsible, at least in part, for the high number of ICs observed at 7 days.

The inflammatory process involves a complex and coordinated cascade of cellular and molecular events that culminate with production and release of several cytokines.[32–34] Among these cytokines, IL-6 is a proinflammatory cytokine that may activate and modulate specific cells and, therefore, exerts an important role in the inflammatory reaction[34] and in the bone resorption.[35] Our findings revealed that the radiopacifier agents promoted a significant increase in the number of IL-6 immunolabeled cells in the capsules. However, this increase was significantly higher in the CS + BO in comparison with CS + ZrO_2. There is strong evidence that IL-6 may stimulate the production of matrix metalloproteinases leading to tissue degradation.[36] Thus, the gradual and significant reduction in the IL-6 immunolabeled cells suggests that the capsules are undergoing an intense remodeling process in the initial periods. In addition, the presence of well-oriented collagen fibers bundles in the capsules indicates that initial inflammatory reaction was almost totally replaced, in the period of 60 days, by a dense connective tissue.

Considering that biocompatibility of the materials depends on the components released and our results revealed that BO associated to CS promoted the highest inflammatory reaction and IL-6 immunolabeled cells, it is possible that the BO acts as an irritant substance. It has been demonstrated that the level of zirconium released in solution is smaller in comparison with the bismuth indicating that the association of ZrO_2 to the PC is more stable than the BO added to the PC.[15]

The sections submitted to von Kossa method exhibited black structures in the capsule adjacent to the tubes filled with the cements, with pattern similar to von Kossa-positive calcified structures described by other authors.[26,28,37] In addition, the sections of long bone from newborn rats used as positive control showed typical trabeculae bone positive to von Kossa, that is, in black color. Thus, these structures may constitute globules containing calcium that were possibly released by CSs. Moreover, von Kossa positive structures were never seen in the capsule adjacent to the empty tubes reinforcing the concept that CS cements are responsible for formation of these von Kossa-positive structures. The deposition of the calcified structures has been reported in response to PC and MTA implanted in the subcutaneous tissue.[26] It is known that CSs reaction give rise to the calcium silicate hydrated gel and calcium hydroxide.[9] Thus, likewise calcium hydroxide, the CS may release calcium ions as shown in this study. The calcium ions can react with carbonate dioxide in the tissues giving rise to calcite crystals. The calcite crystals act as a calcification nucleus and, therefore, could facilitate the mineralization process.[38,39] In fact, MTA induced bone-like tissue formation in perforation of pulp chamber floor experimentally created in rat molars.[2] Moreover, osteopontin was detected in fibroblasts of capsules surrounding the MTA and PC implanted in the subcutaneous.[26] Considering that osteopontin is a glycoprotein highly expressed in mineralized tissues as well as pathologic calcification sites of soft tissues,[40] it has been suggested that MTA and PC could stimulate mesenchymal cells of subcutaneous tissue to express the osteoblast-like phenotype.[26]

CONCLUSION

The present findings indicate that the association of microparticulated or nanoparticulated ZrO_2 provides satisfactory physicochemical and biological properties to the CS. The similar tissue reaction promoted by microparticulated and nanoparticulated ZrO_2 reinforces the idea that ZrO_2 may not interfere in the hydration reaction of CS. So, ZrO_2 may be a good alternative for use as radiopacifying agent in substitution to BO. However, the addition of nanoparticulated radiopacifier did not improve the physicochemical and biological properties of CS when compared with microparticulated ZrO_2.

ACKNOWLEDGMENTS

The authors thank Mr. Luis Antônio Potenza and Mr. Pedro Sérgio Simões for technical support.

REFERENCES

1. Lee SJ, Monsef M, Torabinejad M. Sealing ability of mineral trioxide aggregate for repair of lateral root perforations. J Endod 1993; 19:541–544.
2. Silva GF, Guerreiro-Tanomaru JM, Sasso-Cerri E, Tanomaru-Filho M, Cerri PS. Histological and histomorphometrical evaluation of furcation perforations filled with MTA, CPM and ZOE. Int Endod J 2011;44:100–110.

3. Wucherpfennig AL, Green DB. Mineral trioxide vs. Portland cement: Two biocompatible filling materials. J Endod 1999;25: 308; Abstract No. 40.
4. Wynn-Jones G, Shelton RM, Hofmann MP. Development of Portland cement for orthopedic applications, establishing injectability and decreasing setting times. J Biomed Mater Res Part B 2012: 100B:2213–2221.
5. Bortoluzzi EA, Guerreiro-Tanomaru JM, Tanomaru-Filho M, Duarte MAH. Radiographic effect of different radiopacifiers on a potential retrograde filling material. Oral Surg Oral Med Oral Pathol Oral Radiol Endod 2009;108:628–632.
6. Duarte MAH, El Kadre GDO, Vivan RR, Guerreiro-Tanomaru JM, Tanomaru-Filho M, de Moraes IG. Radiopacity of Portland cement associated with different radiopacifying agents. J Endod 2009;35: 737–740.
7. Duarte MAH, Minotti PG, Rodrigues CT, Ordinola-Zapata R, Bramante CM, Tanomaru-Filho M, Vivan RR, de Moraes IG, de Andrade FB. Effect of different radiopacifying agents on the physicochemical properties of white Portland cement and white mineral trioxide aggregate. J Endod 2012;38:394–397.
8. Coomaraswamy KS, Lumley PJ, Hofmann MP. Effect of bismuth oxide radioopacifier content on the material properties of an endodontic Portland cement-based (MTA-like) system. J Endod 2007;33:295–298.
9. Camilleri J. Hydration mechanisms of mineral trioxide aggregate. Int Endod J 2007;40:462–470.
10. Tanomaru-Filho M, Morales V, Silva GF, Bosso R, Reis JMSN, Duarte MAH, Guerreiro-Tanomaru JM. Compressive strength and setting time of MTA and Portland cement associated with different radiopacifying agents. ISRN Dent 2012;2012:898051.
11. Camilleri J. The physical properties of accelerated Portland cement for endodontic use. Int Endod J 2008;41:151–157.
12. Camilleri J, Montesin FE, Papaioannou S, McDonald F, Pitt Ford TR. Biocompatibility of two commercial forms of mineral trioxide aggregate. Int Endod J 2004;37:699–704.
13. Min KS, Kim HI, Park HJ, Pi SH, Hong CU, Kim EC. Human pulp cells response to Portland cement in vitro. J Endod 2007;33:163–166.
14. Cutajar A, Mallia B, Abela S, Camilleri J. Replacement of radiopacifier in mineral trioxide aggregate; characterization and determination of physical properties. Dent Mater 2011;27:879–891.
15. Camilleri J, Cuttajar A, Mallia B. Hydration characteristics of zirconium oxide replaced Portland cement for use as a root-end filling material. Dent Mater 2011;27:845–854.
16. Komabayashi T, Spangberg L. Comparative analysis of the particle size and shape of commercially available mineral trioxide aggregates and Portland cement: A study with a flow particle image analyzer. J Endod 2008;34:94–98.
17. Saghiri MA, Asgar K, Lofti M, Garcia-Godoy F. Nanomodification of mineral trioxide aggregate for enhanced physiochemical properties. Int Endod J 2012;45:979–988.
18. Liu X, Huang A, Ding C, Chu PK. Bioactivity and cytocompatibility of zirconia (ZrO_2) films fabricated by cathodic arc deposition. Biomaterials 2006;27:3904–3911.
19. Saldaña L, Méndez-Vilas A, Jiang L, Multigner M, González-Carrasco JL, Pérez-Prado MD, González-Martin ML, Munuera L, Vilaboa N. In vitro biocompatibility of an ultrafine grained zirconium. Biomaterials 2007;28:4343–4354.
20. Vivan RR, Ordinola-Zapata R, Zeferino MA, Bramante CM, Bernardineli N, Garcia RB, Duarte MAH, Tanomaru-Filho M, de Moares IG. Evaluation of the physical and chemical properties of two commercial and three experimental root-end filling materials. Oral Surg Oral Med Oral Pathol Oral Radiol Endod 2010;110:250–256.
21. International Organization for Standardization. ISO 6876: Dental Root Sealing Materials. Geneva: The Organization; 2001.
22. American National Standard. American Dental Association Specification n° 57 for Endodontic Filling Materials. Chicago: American Dental Association (ADA); 1984.
23. American Society for Testing and Materials. Standard Test Method for Time and Setting of Hydraulic-Cement Paste by Gillmore Needles, ASTM C266–03. Philadelphia: American Society for Testing and Materials (ASTM); 2000.
24. Bortoluzzi EA, Broon NJ, Bramante CM, Felippe WT, Tanomaru-Filho M, Esberard RM. The influence of calcium chloride on the setting time, solubility, disintegration, and pH of mineral trioxide aggregate and white Portland cement with a radiopacifier. J Endod 2009;35:550–544.
25. International Organization for Standardization. ISO 9917-1: Dentistry—Water-Based Cements—Part 1: Powder/Liquid Acid-Base Cements. Geneva: The Organization; 2003.
26. Viola NV, Guerreiro-Tanomaru JM, Silva GF, Sasso-Cerri E, Tanomaru-Filho M, Cerri PS. Morphological and morphometric analysis of the biocompatibility of an experimental MTA sealer. J Biomed Mater Res Part B 2012;100:1773–1781.
27. Longhini R, de Oliveira PA, Faloni APS, Sasso-Cerri E, Cerri PS. Increased apoptosis in osteoclasts and decreased RANKL immunoexpression in periodontium of cimetidine-treated rats. J Anat 2013;222:239–247.
28. Gomes-Filho JE, Watanabe S, Bernabe PFE, Costa MTM. A mineral trioxide aggregate sealer stimulated mineralization. J Endod 2009;35:256–260.
29. Islam I, Chng HK, Yap AUJ. Comparison of the physical and mechanical properties of MTA and Portland cement. J Endod 2006;32:193–197.
30. Shahi S, Rahimi S, Yavari HR, Mokthari H, Roshangar L, Abasi MM, Sattari S, Abdolrahimi M. Effect of mineral trioxide aggregates and Portland cements on inflammatory cells. J Endod 2010; 36:899–903.
31. Vosoughhosseini S, Lotfi M, Shahi S, Baloo H, Mesgariabbasi M, Ali Saghiri M, Zand V, Rahimi S, Ranjkesh B. Influence of white versus gray mineral trioxide aggregate on inflammatory cells. J Endod 2008;34:715–717.
32. Schroder AK, Ohe M, Kolling U, Altstaedt J, Uciechowski P, Fleischer D, Dalhoff K, Ju X, Zenke M, Heussen N, Rink L. Polymorphonuclear leucocytes selectively produce anti-inflammatory interleukin-1 receptor antagonist and chemokines, but fail to produce pro-inflammatory mediators. Immunology 2006;119:317–327.
33. Hrabak A, Bajor T, Csuka I. The effect of various inflammatory agents on the phagocytosis and cytokine profile of mouse and rat macrophages. Inflam Res 2008;57:75–83.
34. Nibali L, Fedele S, D'Aiuto F, Donos N. Interleukin-6 in oral diseases: A review. Oral Dis 2012;18:236–246.
35. Phan TC, Xu J, Zheng MH. Interaction between osteoblast and osteoclast: Impact in bone disease. Histol Histopathol 2004;19:1325–1344.
36. Wisithphrom K, Windsor LJ. The effects of tumor necrosis factor-alpha, interleukin-1 beta, interleukin-6, and transforming growth factor-beta 1 on pulp fibroblast mediated collagen degradation. J Endod 2006;32:853–861.
37. Katchburian E, Antoniazzi MM, Jared C, Faria FP, Souza Santos H, Freymüller E. Mineralized dermal layer of the Brazilian tree-frog *Corythomantis greeningi*. J Morphol 2001;248:56–63.
38. Seux D, Couble ML, Hartmann DJ, Gauthier JP, Magloire H. Odontoblast-like cytodifferentiation of human dental pulp cells in vitro in the presence of calcium hydroxide cement. Arch Oral Biol 1991;36:117–128.
39. Sarkar NK, Caicedo R, Ritwik P, Moiseyeva R, Kawashima I. Physicochemical basis of the biologic properties of mineral trioxide aggregate. J Endod 2005;31:97–100.
40. Sodek J, Ganss B, McKee MD. Osteopontin. Crit Rev Oral Biol Med 2000;11:279–303.